High performance terahertz quantum cascade laser sources based on intracavity difference frequency generation

Q. Y. Lu, N. Bandyopadhyay, S. Slivken, Y. Bai, and M. Razeghi*

Center for Quantum Devices, Department of Electrical Engineering and Computer Science, Northwestern University, Evanston, IL 60208, USA

** razeghi@eecs.northwestern.edu*

Abstract: We demonstrate high power, room temperature, single-mode THz emissions based on intracavity difference frequency generation from mid-infrared quantum cascade lasers. Dual active regions both featuring giant nonlinear susceptibilities are used to enhance the THz power and conversion efficiency. The THz frequency is lithographically tuned by integrated dual-period distributed feedback gratings with different grating periods. Single mode emissions from 3.3 to 4.6 THz with side-mode suppression ratio and output power up to 40 dB and 65 μW are obtained, with a narrow linewidth of 5 GHz.

OCIS codes: (140.3070) Infrared and far-infrared lasers; (190.4223) Nonlinear wave mixing; (140.5965) Semiconductor lasers; (230.5590) Quantum-well, -wire and -dot devices; (140.3490) Lasers, distributed-feedback.

References and links

1. B. Ferguson and X. C. Zhang, "Materials for terahertz science and technology," Nat. Mater. **1**(1), 26–33 (2002).
2. M. Tonouchi, "Cutting-edge terahertz technology," Nat. Photonics **1**(2), 97–105 (2007).
3. R. Köhler, A. Tredicucci, F. Beltram, H. E. Beere, E. H. Linfield, A. G. Davies, D. A. Ritchie, R. C. Iotti, and F. Rossi, "Terahertz semiconductor-heterostructure laser," Nature **417**(6885), 156–159 (2002).
4. S. Fathololoumi, E. Dupont, C. W. I. Chan, Z. R. Wasilewski, S. R. Laframboise, D. Ban, A. Mátyás, C. Jirauschek, Q. Hu, and H. C. Liu, "Terahertz quantum cascade lasers operating up to ~ 200 K with optimized oscillator strength and improved injection tunneling," Opt. Express **20**(4), 3866–3876 (2012).
5. M. A. Belkin, F. Capasso, F. Xie, A. Belyanin, M. Fischer, A. Wittmann, and J. Faist, "Room temperature terahertz quantum cascade laser source based on intracavity difference-frequency generation," Appl. Phys. Lett. **92**(20), 201101 (2008).
6. Q. Y. Lu, N. Bandyopadhyay, S. Slivken, Y. Bai, and M. Razeghi, "Room temperature single-mode terahertz sources based on intracavity difference-frequency generation in quantum cascade lasers," Appl. Phys. Lett. **99**(13), 131106 (2011).
7. K. Vijayraghavan, R. W. Adams, A. Vizbaras, M. Jang, C. Grasse, G. Boehm, M. C. Amann, and M. A. Belkin, "Terahertz sources based on Čerenkov difference-frequency generation in quantum cascade lasers," Appl. Phys. Lett. **100**(25), 251104 (2012).
8. M. A. Belkin, F. Capasso, A. Belyanin, D. L. Sivco, A. Y. Cho, D. C. Oakley, C. J. Vineis, and G. W. Turner, "Terahertz quantum-cascade-laser source based on intracavity difference-frequency generation," Nat. Photonics **1**(5), 288–292 (2007).
9. Q. Y. Lu, Y. Bai, N. Bandyopadhyay, S. Slivken, and M. Razeghi, "2.4 W room temperature continuous wave operation of distributed feedback quantum cascade lasers," Appl. Phys. Lett. **98**(18), 181106 (2011).
10. M. Geiser, C. Pflügl, A. Belyanin, Q. J. Wang, N. Yu, T. Edamura, M. Yamanishi, H. Kan, M. Fischer, A. Wittmann, J. Faist, and F. Capasso, "Gain competition in dual wavelength quantum cascade lasers," Opt. Express **18**(10), 9900–9908 (2010).

#179357 - $15.00 USD Received 7 Nov 2012; revised 8 Dec 2012; accepted 10 Dec 2012; published 9 Jan 2013

11. S. Slivken, A. Evans, W. Zhang, and M. Razeghi, "High-power, continuous-operation intersubband laser for wavelengths greater than 10 μm," Appl. Phys. Lett. **90**(15), 151115 (2007).
12. P. K. Tien, R. Ulrich, and R. J. Martin, "Optical second harmonic generation in form of coherent Čerenkov radiation from a thin-film waveguide," Appl. Phys. Lett. **17**(10), 447–450 (1970).

1. Introduction

The terahertz (THz) spectral range (λ = 30 ~600 μm) is important for numerous applications in imaging, spectroscopy, and biological engineering [1,2]. It is also the least explored electromagnetic spectral band due to the so-called terahertz gap between electronic devices and photonic devices. THz quantum cascade lasers (QCLs) [3,4] are being developed to provide easier access to this range, yet still need cryogenic cooling. The recent demonstrations of room temperature THz sources based on intracavity difference frequency generation (DFG) [5–7] in mid-infrared (mid-IR) QCLs offers a room temperature solution. For a mid-IR QCL featuring a giant second-order DFG nonlinear susceptibility ($|\chi^{(2)}|$) in its active region and dual wavelength operation, THz emission can be generated within an extremely compact device at room temperature. When dual single-mode operation (λ_1 and λ_2) is generated by a proper spectral purification mechanism, e.g., dual-period distributed feedback (DFB), the THz power $W(\lambda)$ can be expressed as [6,8]:

$$W(\lambda) = \frac{\pi^2 \omega^2 |\chi^{(2)}|^2 W_1 W_2^2 l_{coh}^2}{2\varepsilon\lambda_0 c n n_1 n_2 S_{eff}}, \quad (1)$$

where $l_{coh} = 1/[|k_i - k_j - k|^2 + (\alpha/2)^2]^{1/2}$ is the coherence length, W_i, n_i, k_i are the mid-IR power, refractive index, and wavenumber at a specific wavelength λ_i (i = 1,2). $\lambda = 1/(1/\lambda_1 - 1/\lambda_2)$ is the generated THz wavelength. n and α are the refractive index and waveguide loss for THz, and S_{eff} is the effective area of interaction. For a given QCL waveguide, the THz power strongly relies on high power mid-IR sources (W_1, W_2), giant $|\chi^{(2)}|$, and better modal interaction between the mid-IR and THz. For most of the THz applications, high power, narrow-linewidth, widely tunable THz sources are desirable. Here the dual active regions both featuring giant nonlinear susceptibilities are used to enhance the THz power and conversion efficiency. Room temperature THz emissions from 3.3 to 4.6 THz based on intracavity DFG in mid-IR QCLs are demonstrated with side-mode suppression ratio (SMSR) and THz power up to 40 dB and 65 μW, respectively, and a narrow linewidth of 5 GHz.

2. Design, growth and fabrication of THz QCL sources based on DFG

The QCL structure was grown by gas-source molecular beam epitaxy on an n-InP substrate (Si, ~1.5×10^{17} cm^{-3}). The growth started with a 5-μm InP buffer layer (Si, ~2×10^{16} cm^{-3}). The laser cores consist of 30 stages of single-phonon resonance (SPR) structures designed for the wavelength of λ_1~9.0 μm, a 100-nm InGaAs spacer (Si, ~2×10^{16} cm^{-3}), and another 30 stages of SPR structure designed for the wavelength of λ_2~10.2 μm. Both active sections feature giant nonlinear susceptibilities of $|\chi^{(2)}| = 3.8\text{-}4.0 \times 10^4$ pm/V for DFG at high operating fields where

#179357 - $15.00 USD Received 7 Nov 2012; revised 8 Dec 2012; accepted 10 Dec 2012; published 9 Jan 2013

maximum mid-IR powers are expected. The growth ended with a 3.5-μm InP cladding layer (Si, ~2×10^{16} cm^{-3}) and a 200-nm InP contact layer (Si, ~5×10^{18} cm^{-3}). Figure 1(a) shows the mid-IR and THz vertical mode distributions. Compared with Refs [5] and [6], where only one of the two active cores is designed with a giant nonlinear susceptibility, the modal interaction area S_{eff} in this structure is improved by a factor of 2 due to the DFG nonlinearities in both active structures, As such, This will contribute to the THz conversion efficiency improvement according to the Eq. (1).

A row of ten devices with dual-period DFB gratings spanning a DFG frequency range from 3.3 to 4.6 THz are defined by electron beam lithography. The gratings were transferred into the cap layer with a grating depth of 200 nm, following the process in Ref [9]. Figure 1(b) is the scanning electron microscope (SEM) image of the grating shape after dry etching. The Fourier analysis of the extrapolated grating shape from the SEM picture shown in the inset of Fig. 1(b) gives two distinct peaks with a THz energy spacing around 4 THz. The other two satellite peaks with the same energy spacing away from the two main peaks correspond to the high-order Fourier series of the grating shape. The sample was processed into double-channel geometries with a 16-μm ridge width tapered into 60 μm with a taper angle of 1° toward one end. A narrow ridge width is crucial to secure operation in the fundamental transverse mode, which is then amplified in the tapered region. This is important to the THz generation based on DFG, because an optimal effective area of interaction is expected when both mid-IR wavelengths operate in the fundamental transverse modes. Any higher order mode will significantly reduce the THz signal intensity [10]. The surface grating is defined in the non-tapered region. The device with 3-mm cavity length is high-reflection (HR) and anti-reflection (AR) coated with Si_3N_4/Au (400/1000 nm) and Y_2O_3 (1000 nm), respectively.

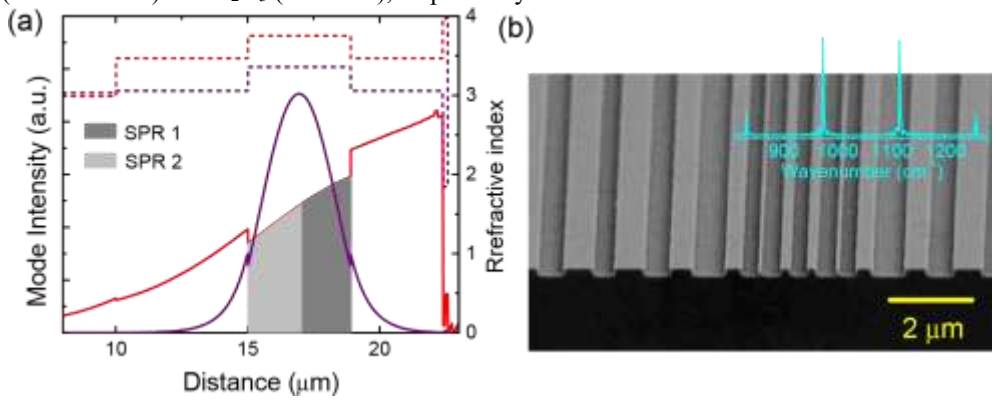

Fig. 1. (a) Mid-IR and THz vertical mode and index distributions (dashed lines). The shadowed areas represent the THz confinement in the active regions. (b) SEM image of a dual-period grating after dry etching. Inset: Fourier analysis of the corresponding gratings.

All testing was performed at room temperature in pulsed mode operation, with a pulse width of 60 ns and a duty cycle of 1.5%. The THz power measurement system is similar to Ref [6]. Optical filters were used to differentiate the THz power from mid-IR powers. Spectral measurements were performed with a Bruker Fourier transform infrared (FTIR) spectrometer equipped with a mercury-cadmium-telluride (MCT) photodetector for mid-IR and a liquid helium-cooled silicon bolometer for THz signals. The far fields were obtained with a computer controlled rotational stage and a MCT detector.

#179357 - $15.00 USD Received 7 Nov 2012; revised 8 Dec 2012; accepted 10 Dec 2012; published 9 Jan 2013

3. Experimental results and discussions

The highest THz output power is obtained from a device operating at 4 THz. Figure 2 shows the mid-IR and THz performances for this device. The mid-IR spectra and electroluminescence (EL) spectrum from a reference mesa structure are shown in Fig. 2(a). Considering that the free-carrier absorption in the waveguide has a λ^2 dependence [11], the mid-IR spectra are intentionally blue shifted by ~35 cm^{-1} with respect to the gain peak for a better power balance between the two wavelengths. Primary emissions at $\lambda_1 = 9.0$ μm and $\lambda_2 = 10.22$ μm are obtained at all working currents. The other two nontrivial emissions at $\lambda_1' = 8.06$ μm and $\lambda_2' = 11.85$ μm are attributed to the high-order Fourier series of the grating shape as shown in the inset of Fig. 1(b). The power-current-voltage (*P-I-V*) characterizations for the two wavelengths are shown in Fig. 2(b). Compared with results in Ref [6], the total power is enhanced by a factor of 2 and the input electrical power is reduced by about 40%. A proper optical filter is used to differentiate the two mid-IR wavelengths λ_1 and λ_2. The measured powers for λ_1 and λ_2 shown in Fig. 2(b) include the roughly 5% contributions from λ_1' and λ_2', which are estimated by comparing the peak intensities in the emitting spectra. The far fields (inset of Fig. 2(b)) of the total mid-IR output are single lobed and nearly diffraction-limited, which indicates that all the wavelengths are working in their fundamental transverse modes.

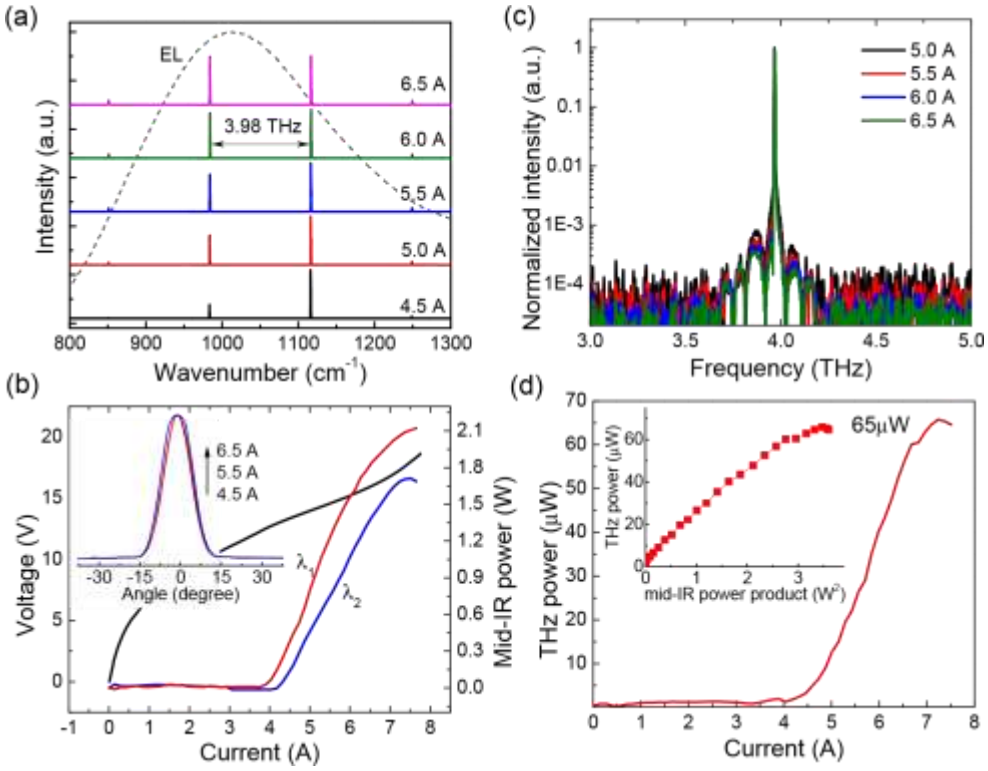

Fig. 2. Room temperature mid-IR and THz characteristics of a device operating at 4 THz. (a) Mid-IR spectra at different currents and EL spectrum from a reference mesa structure. (b) *P-I-V* characterization for the two wavelengths. Inset: far fields at different currents. (c) THz power as a function of current and mid-IR-power products (inset). (d) Normalized THz spectra at different currents.

#179357 - $15.00 USD Received 7 Nov 2012; revised 8 Dec 2012; accepted 10 Dec 2012; published 9 Jan 2013

Figure 2(c) shows the THz spectra measurement results. The device exhibits stable single mode operation around 4 THz (λ ~75.4 μm). The spectrum linewidth is about 5 GHz, which is mainly limited by the resolution of the FTIR (0.125 cm^{-1}). The SMSR is as high as 40 dB at high currents (>6.0 A), and the THz spectral position is very stable as the current changes. The THz current tuning rate is 0.60 GHz/A, which is about one order of magnitude smaller than the mid-IR tuning rates (5.4 and 6.0 GHz/A for λ_1 and λ_2). This indicates that the THz emission is relatively insensitive to current or temperature fluctuations, which is beneficial for many applications.

Figure 2(d) shows the THz power and mid-IR-power product at room temperature. The THz power measurement system is purged with nitrogen flow to reduce the water vapor absorption. A maximum THz peak power of 65 μW is obtained. The THz power conversion efficiency is about 30 $\mu W/W^2$ near threshold, and 23 $\mu W/W^2$ at high currents. Since the THz DFG is featured in both cores, the effective area of modal interaction is estimated to be about $S_{eff} \approx 2 \times 10^3$ μm^2. Given the waveguide is designed to be nearly phase-matched, and has an estimated coherence length l_{coh} ~120 μm, a THz power conversion efficiency of 110 $\mu W/W^2$ is expected. This discrepancy can be attributed to the following factors. On one side, the water vapor transmittance measurement in THz range shown in Fig. 3(b) (upper panel) indicates that there is a strong absorption line at this wavelength. Even with the nitrogen purging, there is still some water vapor residue that contributes to the absorption of THz light. On the other hand, the Si lens used for collimation also reflects some portion of the THz light. Since the index of Si is about 3.42, nearly 30% of the THz light is reflected backward to the laser at the Si/air interface. An AR coating (e.g., a layer of polyethylene) deposited to the Si lens would be able to couple out the THz light more efficiently and further enhance the THz power close to 100 μW.

#179357 - $15.00 USD Received 7 Nov 2012; revised 8 Dec 2012; accepted 10 Dec 2012; published 9 Jan 2013

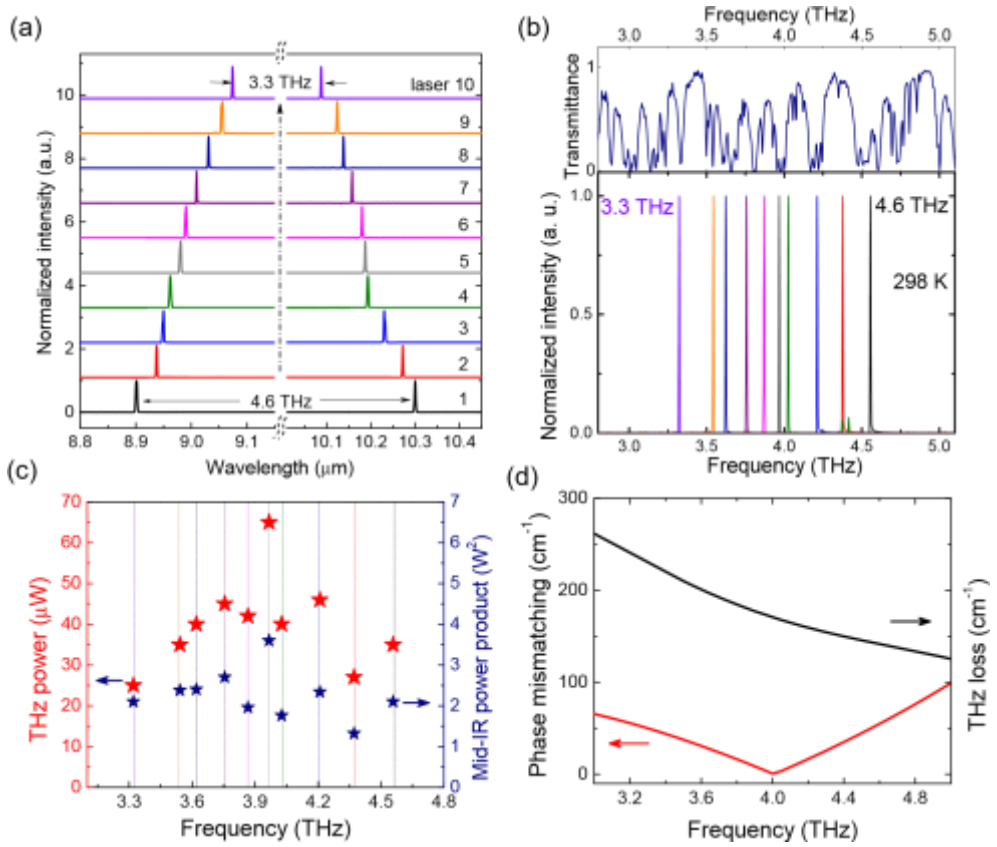

Fig. 3. (a) Mid-IR spectra of a row of ten DFB devices with varied DFG frequencies. (b) The THz spectra of the devices emitting from 3.3 to 4.6 THz (lower panel), and the water transmittance spectra taken with FTIR under a relative humidity around 30% (upper panel). (c) THz powers and mid-IR power products of the devices emitting at different THz frequencies. The dashed lines are used for guidance. (d) Calculated phase mismatching between mid-IR and THz modes and the THz waveguide losses as a function of THz wavelength.

A row of ten devices with dual-period DFB gratings designed with varied THz frequencies are tested and characterized. Figure 3(a) shows the mid-IR spectra from different DFB grating designs at room temperature. The frequency spacing between the two wavelengths λ_1 and λ_2 changes from 110 to 153 cm^{-1}. As a result, single mode operations spanning a spectral range of 3.3-4.6 THz from these devices are demonstrated, as shown in Fig. 3(b) (lower panel), with a tuning range of 1.3 THz and a mean SMSR above 30 dB. The water vapor absorption measurement result shown in Fig. 3(b) (upper panel) indicates that there are strong absorptions for some emitting wavelengths. Figure 3(c) shows the maximum THz powers and mid-IR power products for each frequency. The THz power and conversion efficiency both peak at 4 THz with 65 μW and 23 $\mu W/W^2$ respectively, and decrease to 25 μW and 11 $\mu W/W^2$ at 3.3 THz. The varied power conversion efficiencies are mainly attributed to the wavelength-dependent phase mismatching and waveguide loss, as shown in Fig. 3(d). While the mid-IR and THz modes are nearly modal-phase matched around 4 THz, their modal phases become increasingly mismatched as the THz frequency shifts away from the matching condition. Besides, the THz loss increases rapidly as THz frequency decreases from 5 to 3 THz. The overall contribution from these effects makes the THz power conversion efficiency varying

#179357 - $15.00 USD Received 7 Nov 2012; revised 8 Dec 2012; accepted 10 Dec 2012; published 9 Jan 2013

significantly in this range. THz generation outside of this range becomes less efficient due to the narrow band modal phase matching scheme. While the broad-band Čerenkov phase matching strategy will be able to further widen this step tuning range.[7,12], high THz power is still able to be demonstrated by modal phase matching scheme thanks to higher mid-IR powers, effective heating removal with thinner substrate and uniform current injection. By further optimizing the phase matching scheme, waveguide geometry, and pump powers, mW-level THz powers should be achievable at room temperature.

4. Conclusion

In conclusion, we demonstrate high power, room temperature, single-mode THz emissions based on intracavity DFG in mid-IR QCLs. The THz frequency is lithographically tuned by integrated dual-period DFB gratings with different grating periods. Narrow linewidth, single mode emissions from 3.3 to 4.6 THz with side-mode suppression ratio and output power up to 40 dB and 65 μW are obtained.

Acknowledgments

This work is partially supported by the National Science Foundation under grant ECCS-1231289. The authors would also like to acknowledge the encouragement and support of Dr. K.K. Law from the Naval Air Warfare Center, Dr. T. Manzur from the Naval Undersea Warfare Center, and Dr. N. Dhar from the Defense Advanced Research Projects Agency.

#179357 - $15.00 USD Received 7 Nov 2012; revised 8 Dec 2012; accepted 10 Dec 2012; published 9 Jan 2013